ELSEVIER

Biochimica et Biophysica Acta 1414 (1998) 31–42

BIOCHIMICA ET BIOPHYSICA ACTA
BBA

Kinetics of the interactions of a dicarboxylic porphyrin with unilamellar lipidic vesicles: interplay between bilayer thickness and pH in rate control

Nathalie Maman, Daniel Brault *

Laboratoires de Photobiologie et de Biophysique, CNRS UA 481, INSERM U. 201, Muséum National d'Histoire Naturelle, 43 rue Cuvier, 75231 Paris Cedex 05, France

Received 10 June 1998; accepted 4 August 1998

Abstract

The transfer of a dicarboxylic porphyrin from phosphatidylcholine fluid-phase unilamellar vesicles towards albumin is studied focusing on bilayer thickness and pH effects. The kinetics of this process yield the rate constants for the porphyrin flip-flop from the inner to the outer hemileaflet and its exit towards aqueous medium. Phospholipids with monounsaturated 14–22 carbon chains are used. Interplay between bilayer thickness and pH for the control of the rate constants is observed. This results in the amplification, at physiological pH, of the effect of membrane thickness on the flip-flop and exit rates as compared to pH 8.5 and 6.5. These data are explained by the degree of porphyrin burying within the bilayer resulting from a compromise between favorable hydrophobic interactions with the hydrocarbon phase and unfavorable penetration of the polar carboxylic chains. The balance between the two effects depends particularly on the neutralization of one carboxylic chain. Considering the bilayer hydrophobicity profile and the porphyrin size, the optimization of hydrophobic interactions appears dependent on the bilayer thickness. The flip-flop and the exit are governed by neutralization and deprotonation of the carboxylic chains, respectively, the rate of these proton exchanges being dependent on the porphyrin location within the bilayer.

Keywords: Porphyrin; Bilayer; Thickness; Kinetics; Permeability; pH

1. Introduction

Photodynamic therapy (PDT) is based on the generation of very toxic short-lived species, such as singlet oxygen, upon absorption of light by photosensitizing agents [1]. These processes are exploited in therapy of tumors which accumulate photosensitizers, in particular porphyrins, to some extent [2]. A dual selectivity results from the photosensitizer retention and the possibility to restrict the light irradiation to the tumor site. Although various mechanisms come into play in tumor photoinactivation [3], the direct photosensitization of tumor cells is of obvious importance. Owing to their brief lifetime, the reactive species produced through light irradiation poorly diffuse in a biological environment. This diffusion has been estimated to less than 0.1 μm for singlet oxygen [4]. Thereby, only subcellular structures labeled by the photosensitizer are damaged after lightening. As a matter of fact, a significant

* Corresponding author. Fax: +33 (1) 4079-3705; E-mail: brault@mnhn.fr

0005-2736/98/$ – see front matter
PII: S0005-2736(98)00149-7

correlation is observed between the phototoxicity and the localization of the drug in some organites [5]. Moreover, the mechanism of photosensitized cell death (apoptosis versus necrosis) has been recently shown to depend on the subcellular photosensitizer localization [6,7]. The partition of the photosensitizer among subcellular structures involves permeation through membranes, a time-dependent process. Thus, a precise knowledge of the factors governing the diffusion of these molecules across membranes is likely to contribute to the improvement of PDT. This problem also has obvious relevance to the biosynthesis of heme which involves transfer of protoporphyrin and its iron complex through the inner mitochondrial membrane.

In order to gain insight into these processes, membrane models consisting in unilamellar vesicles have been developed [8–16]. We focused on a dicarboxylic porphyrin, deuteroporphyrin (DP), because its structure corresponds to the framework of the components of Photofrin, the only drug with approval to date. In line with studies on the membrane transport of heme [9,11] or drugs such as antibiotics [17], a method based on the scavenging of the permeant molecule by a macromolecule located on one side of the bilayer was developed. Albumin was chosen for its high affinity for porphyrins [18]. Deuteroporphyrin was found to preferentially locate in each hemileaflet with its carboxylic chains oriented towards the water interface [15,19]. The steps corresponding to the exit of the porphyrin from the outer leaflet of the bilayer and to its flip-flop between the two layers were characterized by using fluorescence spectroscopy.

The rate constants for the exit of the porphyrin from the outer layer and for its flip-flop were strongly affected by the physical state of the lipidic bilayer which was modulated by the presence of cholesterol and by temperature [15]. Through the control of the ionization state of the porphyrin carboxylic chains, pH had a drastic effect on the two rate constants [14]. The exit of the dianionic form (deprotonated chains) was accelerated while the reverse effect was observed for its flip-flop. Thus, the limiting step in the transfer of the porphyrin through membranes appears to be the passage of its polar chains through the hydrophobic region of the bilayer. It was recently shown [20] that unsaturated phospholipids provide better hydrophobic barriers than the saturated forms. In any case, the size of the effective hydrophobic barrier does not exceed 50% of the thickness of the hydrocarbon phase [20,21]. In this respect, the size of deuteroporphyrin must be considered (see Fig. 1). It is an amphiphilic molecule with a tetrapyrrolic hydrophobic core of about 12 Å diameter and two polar side chains extending on one side. The total distance between the oxygens of a carboxylate group and the methyl on the opposite pyrrole is 14 Å. For comparison, the hydrocarbon thickness of liposomes made of C14 saturated chains is about 23 Å [22] which makes the actual size of the hydrophobic barrier close to the porphyrin dimension. Thus, it can be expected that the interactions of this porphyrin with membranes will be greatly dependent on the thickness of the bilayer. In the present paper, we investigate this problem by using phosphatidylcholine unilamellar vesicles with fatty acid chains comprising 14–22 carbon atoms. In order to mimic more accurately biological membranes and to allow comparison between vesicles in the same state, chains with one double bond (*cis* isomer) were selected. This series of monounsaturated lipids remains in the liquid crystalline state at the temperature used.

Subtle correlations were found between the effects of pH and bilayer thickness. These effects are accounted for by the degree of burying of the porphyrin within the bilayer which depends both on hydrophobic interactions between the porphyrin core and the lipid phase and, on the ionization of the carboxylic chains.

2. Materials and methods

2.1. Measurements

Emission spectra and slow kinetics (time >30 s) were measured using a SPEX spectrofluorometer (Edison, NJ). Fast kinetic measurements (time <10 s) were performed with the aid of a Durrum–Gibson stopped-flow apparatus (Palo Alto, CA) with a mixing time of 3 ms. The excitation light provided by a 75 W short-arc xenon lamp was passed through a monochromator set at 389 nm. Fluorescence emission was collected above 610 nm using a low-cut filter (Schott OG 610, Mainz, Germany) which re-

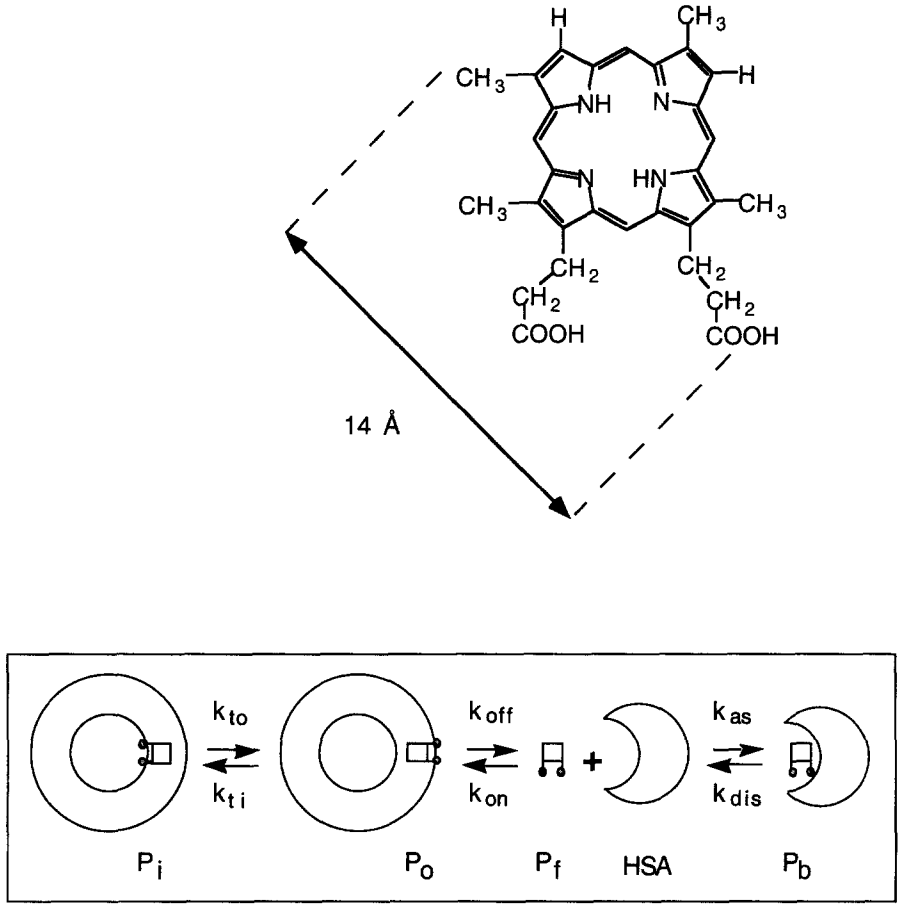

Fig. 1. Structure of deuteroporphyrin (neutral form) and scheme for its transfer from vesicles to albumin.

moves the scattered light. The signal was recorded using an oscilloscope (Nicolet Model 3091, Madison, WI) and then fed to a computer (Hewlett-Packard Model 9816, Fort Collins, CO). The signals were fitted by mono- or bi-exponential curves using a program based on the least-square method as explained elsewhere [15]. All the measurements were performed at 25°C. The size of the vesicles was determined by quasi-elastic light scattering using a Coulter N4 Plus analyzer (Hialeah, CA).

2.2. Materials

Deuteroporphyrin, was prepared in our laboratory and its purity checked to be better than 99% by HPLC [23]. Lipid free human serum albumin (HSA) was purchased from Sigma (St. Louis, MO). The vesicles were prepared using the following unsaturated phospholipids: dimyristoleoyl-(C14:1); dipalmitoleoyl-(C16:1); dioleoyl-(C18:1); dieicosanoyl-(C20:1); and dierucoyl-(C22:1) phosphatidylcholines. They were obtained from Avanti Polar Lipids (Alabaster, AL) as chloroformic solutions.

2.3. Sample preparation

All the experiments were performed using 0.15 M NaCl solutions buffered to various pH values (6.5–8.5) with phosphate (20 mM) or Tris (20 mM). Small unilamellar vesicles were prepared by extrusion [24,25]. The lipid solutions in chloroform were taken to dryness and then dispersed in buffer by vortexing. The resulting liposome suspension was extruded 8–10 times through a stack of polycarbonate membrane filters (Poretics, Livermore, CA) with pores of 50 nm using an extruder device (Lipex Biomembranes, Vancouver, Canada) thermostated at 25°C. The distribution of the size of the vesicles thus prepared was

fairly homogeneous as determined by quasi-elastic light scattering. The standard deviation on the population was found to be around 20 nm using unimodal analysis. The vesicle diameter slightly increased with the phospholipid chain length (from about 65 nm for the C14 chains to 79 nm for the C22). No significant change in the diameter was found over the pH range investigated. In all the kinetics experiments, vesicles preloaded with porphyrin were used. In this case, a solution of deuteroporphyrin dissolved in tetrahydrofuran was added to the lipid solution in chloroform prior to the evaporation step. After dissolution of HSA in buffer, the pH was eventually adjusted to the desired values (± 0.01 unit).

2.4. Kinetics of the transfer of deuteroporphyrin from vesicles to albumin

Vesicles preloaded with DP as described above were mixed either in the stopped-flow apparatus or by hand, depending on the transfer rate, with solutions of albumin. The final porphyrin concentration was 1×10^{-7} M. A scheme describing the various steps involved in the transfer is shown in Fig. 1. The porphyrin loaded in the vesicles distributes between the inner (P_i) and the outer hemileaflet (P_o). On mixing with the albumin (HSA), all the equilibria are shifted to allow the binding of the porphyrin (P_b) to the protein leading to fluorescence changes (see Section 3. Although the transfer involves the free porphyrin in the aqueous phase (P_f), its concentration can be kept very low by using vesicle and albumin concentrations high enough. In these conditions, the transfer follows two exponential kinetics as previously established [15]. Intrinsic rate constants characterize the various steps: k_{on} for porphyrin binding to the outer vesicle layer, k_{off} for the exit from the outer layer, k_{ti} for the flip-flop towards the inner and k_{to} towards the outer hemileaflet, k_{as} for the association of the porphyrin to albumin and k_{dis} for its dissociation. The corresponding experimental rate constants for the fast and slow steps, k_1, k_2 respectively, are functions of the intrinsic rate constants [15] as follows:

$$k_{1,2} = (\alpha+\beta+\gamma+\delta \pm [(\alpha+\beta+\gamma+\delta)^2 - 4(\alpha\gamma+\beta\delta+\alpha\delta)]^{1/2})/2 \quad (1)$$

where

$$\alpha = k_{to}$$

$$\beta = k_{ti}$$

$$\gamma = (k_{off}\, k_{as}[HSA])/(k_{on}[LIP] + k_{as}[HSA])$$

$$\delta = (k_{on}\, k_{dis}[LIP])/(k_{on}[LIP] + k_{as}[HSA])$$

In the present work, the effects of the bilayer thickness and the charge of the porphyrin on its exit from the vesicles (k_{off}) and on its movement from the inner to the outer hemileaflet (k_{to}) are examined. In most cases, the flip-flop of the porphyrin was slower than its exit from the vesicles. As previously shown [14,15], the intrinsic rate constants k_{off}, k_{ti}, k_{to}, k_{as} and k_{dis} can be obtained from series of experiments performed with a fixed lipid concentration and various albumin concentrations. The observed rate constants k_1 and k_2 are fitted among the whole range of albumin concentration according to relation 1 and the intrinsic rate constants computed by non-linear regression using the Levenberg–Marquardt algorithm. The Kaleidagraph software (Synergy software, Reading, PA) was used to this end. This procedure was repeated for each pH and each phospholipid used. It is interesting to note that the extrapolation of the curves to extreme values of albumin concentration provides direct estimation of some intrinsic rate constants. The extrapolation of the rates corresponding to the fast and the slow exponential to a zero albumin concentration yields k_{dis} and $k_{ti}+k_{to}$, respectively. Similarly, for the highest albumin concentrations, the fast and the slow exponential yield $k_{off}+k_{ti}$, and k_{to}, respectively. Moreover, for all the experiments performed at the same pH (i.e. whatever the phospholipid may be), the values of k_{as} and k_{dis} remain the same. These considerations greatly help in choosing the initial guesses for the unknown parameters to be determined by the regression software.

In some of our experiments, the porphyrin flip-flop was too slow to be detected with the stopped-flow apparatus and was studied using manual mixing and standard spectrofluorometry. Thereby, the fast phase governed by the exit of the DP from the outer layer and the slow phase corresponding to its flip-flop, were analyzed independently as monoexponentials.

In this case, the experimental rate constant for the fast kinetics obtained by stopped-flow reduces to:

$$k = \gamma + \delta = (k_{off}\ k_{as}[HSA] + k_{on}\ k_{dis}[LIP])/(k_{on}[LIP] + k_{as}[HSA]) \quad (2)$$

At high albumin concentration, the fast rate constant extrapolates to k_{off} (k_{ti} is negligible). The outer hemileaflet is totally depleted from porphyrin after the fast step provided the albumin concentration is high enough. Then, the slowest kinetics correspond to the transfer of the porphyrin from the inner to the outer hemileaflet (k_{to}) that becomes the rate-limiting step. This approximation was used by other authors previously [9,11].

In some cases, the flip-flop was too slow to be investigated by stopped-flow owing to the poor stability of the baseline for times exceeding 10 s and too fast to be feasible by using manual mixing and standard spectrofluorometry.

In some conditions (low pH, short chain phospholipids), the rates for the exit of the porphyrin and for its flip-flop are of the same order of magnitude. As mentioned in a previous paper [14], 'pH-jump experiments' were used to determine the rate constant k_{to} in this pH range. In these experiments, the pH of the albumin solution was adjusted to a higher value than that of the vesicle solution. After mixing in the stopped-flow apparatus, the pH of the bulk aqueous solution (pH_o) reached an intermediate value between the initial pH values of the albumin and vesicle solutions. Then, the pH values were different outside (pH_o) and inside (pH_i) the vesicles, pH_i being equal to the initial pH of the vesicle solution. As the exit of the porphyrin is accelerated when the pH of the bulk aqueous solution is increased (see Section 3), a convenient choice of the pH of the solutions before mixing, makes it possible to separate the two steps and to observe biphasic kinetics [14]. Then, the rate constants k_{off} at pH_o and k_{to} at pH_i can be determined as previously by extrapolation to the highest albumin concentrations.

2.5. Partition experiments

The partition of DP between the aqueous phase and the vesicles was studied by recording the fluorescence emission spectra of series of solutions with various phospholipid concentrations as already described [15,26]. The data were plotted according to the relation

$$F = F_0 + (F_\infty - F_0)\ K_L[LIP]/(1 + K_L[LIP]) \quad (3)$$

where F_0, F_∞ and F are the fluorescence intensities corresponding to no, total and intermediate incorporation of the porphyrin in the vesicles, respectively.

3. Results

3.1. Steady-state measurements

The fluorescence emission spectra of DP in buffer, incorporated in dioleoylphosphatidylcholine vesicles or bound to HSA are shown in Fig. 2. The two latter spectra were obtained using a large excess of either vesicles ([LIP] = 2 10^{-4} M) or albumin ([HSA] = 10^{-5} M), respectively. The excitation wavelengh was set at 396 nm which corresponds to the maximum of excitation for the porphyrin incorporated into the vesicles. The fluorescence spectra of DP appear to be sensitive enough to the environment to easily monitor its transfer from the vesicles to albumin. The fluorescence properties of DP incorporated in vesicles or bound to albumin was independent of pH between 6.5 and 8.5.

Studies on the partition of DP between the aqueous phase and the vesicles were restricted to pH 8.5.

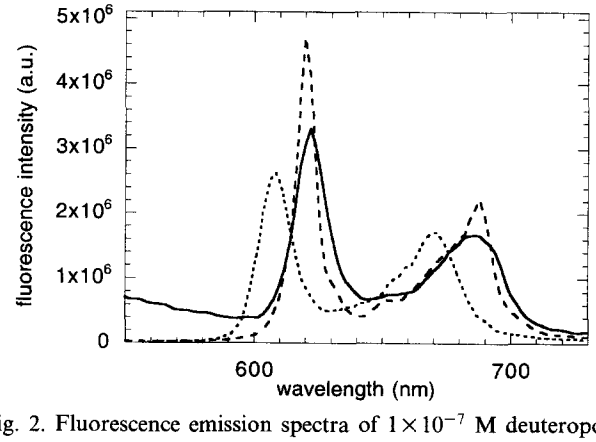

Fig. 2. Fluorescence emission spectra of 1×10^{-7} M deuteroporphyrin in different environments at 25°C, excitation wavelength 396 nm: ···, aqueous solution buffered at pH 8.5; – – –, vesicle solution, [C18:1] = 2×10^{-4} M; ——, albumin solution, [HSA] = 1×10^{-5} M.

The fluorescence spectra were recorded soon after mixing the porphyrin and the vesicle solutions. Under these experimental conditions, the flip-flop of the porphyrin does not take place and only the partition between the aqueous phase and the outer hemileaflet of the vesicles has to be considered. The values of the equilibrium constant K_L for the various phospholipids used are given in Table 1. They refer to the bulk concentration of the phospholipids in the solution which is the most directly accessible parameter. However, only the fraction of lipids in the outer hemileaflet was considered. It was calculated from the vesicle size and the bilayer thickness.

3.2. Kinetics of the transfer of DP from vesicles to albumin

3.2.1. Standard experiments

These experiments involved mixing of solutions of vesicles preloaded with the porphyrin and albumin prepared at the same pH. The concentrations of the porphyrin and the phospholipids after mixing were 1×10^{-7} and 9.8×10^{-5} M, respectively. They were kept constant in all experiments. The transfer was followed by fluorescence. A decay was observed with a maximum amplitude when the excitation wavelength was set at 389 nm. Typical curves and their analysis can be found in a previous study [15]. When the kinetics were clearly biexponential, the intrinsic rate constant for the exit of the porphyrin from the bilayer (k_{off}) and that for its movement from the inner leaflet to the outer one (k_{to}) were obtained from the dependence of the observed rate constants for the fast and slow phases on the albumin concentration using Eq. 1. An example is given in Fig. 3. In keeping with previous studies [14,15],

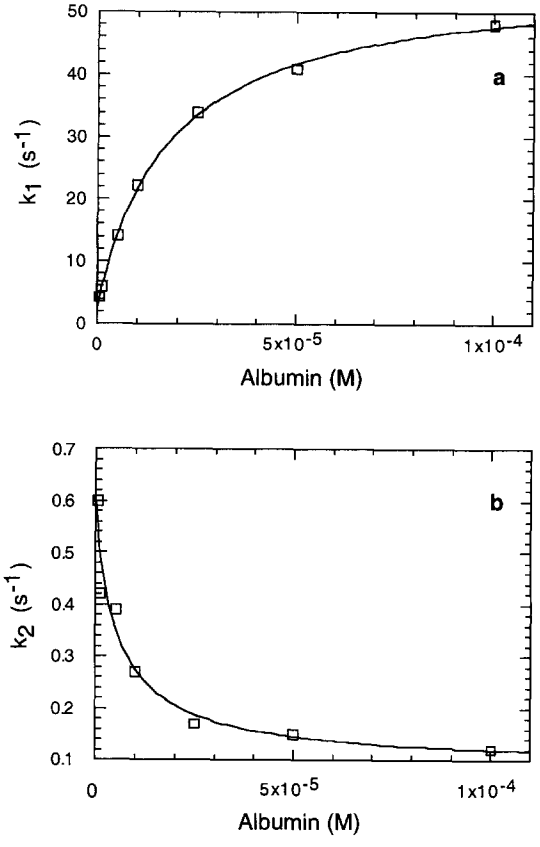

Fig. 3. Transfer of deuteroporphyrin from C14:1-phosphatidylcholine vesicles to albumin: dependence of the experimental rate constants on albumin concentration. Temperature: 25°C. Each point corresponds to the mean calculated from 10 to 20 rate constant determinations. [C14:1] = 9.8×10^{-5} M, [DP] = 1×10^{-7} M. (a) Fast phase and (b) slow phase at pH 7.4 (phosphate buffer). The full lines are theoretical curves according to Eq. 1.

k_{off} was calculated assuming that the values of k_{to} and k_{ti} were the same. In any case, as the flip-flop was slow as compared to the exit, this assumption has little consequence.

Table 1
Interactions of deuteroporphyrin with phosphatidylcholine fluid-phase unilamellar vesicles: selected data

	C14:1		C16:1		C18:1		C20:1		C22:1	
Hydrophobic thickness (Å)	20.0		23.5		27.0		30.5		34.0	
Phosphate distance (Å)	31.0		34.5		38.0		41.5		44.0	
pH	8.5	6.5	8.5	6.5	8.5	6.5	8.5	6.5	8.5	6.5
K_L (M^{-1})[a]	5.5×10^4		7.2×10^4		7.2×10^4		9×10^4		9×10^4	
k_{off} (s^{-1})	52	17	52	14	50	10	53	5	54	4
k_{to} (s^{-1})	8×10^{-4}	2.3	3×10^{-4}	1.7	2×10^{-4}	0.8	1×10^{-4}	0.6	9×10^{-5}	0.4

[a] K_L refers to lipids in the outer hemileaflet.

3.2.2. pH-jump experiments

As the fast phase of the transfer kinetics slowed down and the slow one accelerated with decreasing pH, it was no longer possible to distinguish them at pH 6.5 for all the phospholipids we used (even at pH 6.8 for C14:1). Therefore, pH-jump experiments were designed as described in the Section 2. The validity of this method had been checked experimentally in a previous study [14]. For example, in order to determine k_{to} at pH 6.5 in the case of vesicles made with C14:1, the pH was adjusted to 6.5 for the vesicle solution and to 8.1 for the albumin solution. The pH of the 1:1 mixture of the two solutions was measured to be 7.4. Thereby, after mixing in the stopped-flow apparatus, the pH of the bulk aqueous solution rapidly shift to 7.4 (the change occurs within the mixing time) whereas the original value (6.5) was maintained inside the vesicles. Therefore, the exit rate of the porphyrin from the outer leaflet was accelerated (it corresponds to a pH of 7.4) and a well-defined second phase related to the k_{to} value at pH 6.5 was observed.

3.3. Effects of the bilayer thickness and pH on the kinetics

By using the different methods described above, series of data relating k_{off} and k_{to} to the pH and to the bilayer thickness were obtained. Two buffers were used: phosphate and Tris. Although the buffer power of phosphate was poor around pH 8.5, it was used for comparison. The bilayer thickness was varied using C14–C22 phospholipids. The total thickness (distance between phosphate) and the thickness of the hydrocarbon region indicated in Table 1 were taken from the data of Lewis and Engelman or estimated from the linear dependence between the bilayer thickness and the number of carbons observed by these authors [22].

Fig. 4 shows the dependence of k_{off} and k_{to} on the acyl chain length for three different pH values and two buffers. Both pH and bilayer thickness have a profound effect on the rates. Considering the extreme values, k_{off} is found to span more than one order of magnitude. The effect on k_{to} is considerable: it reaches more than four orders of magnitude. On examination of Fig. 4, a salient feature comes to light: the complex interplay between pH and thickness for

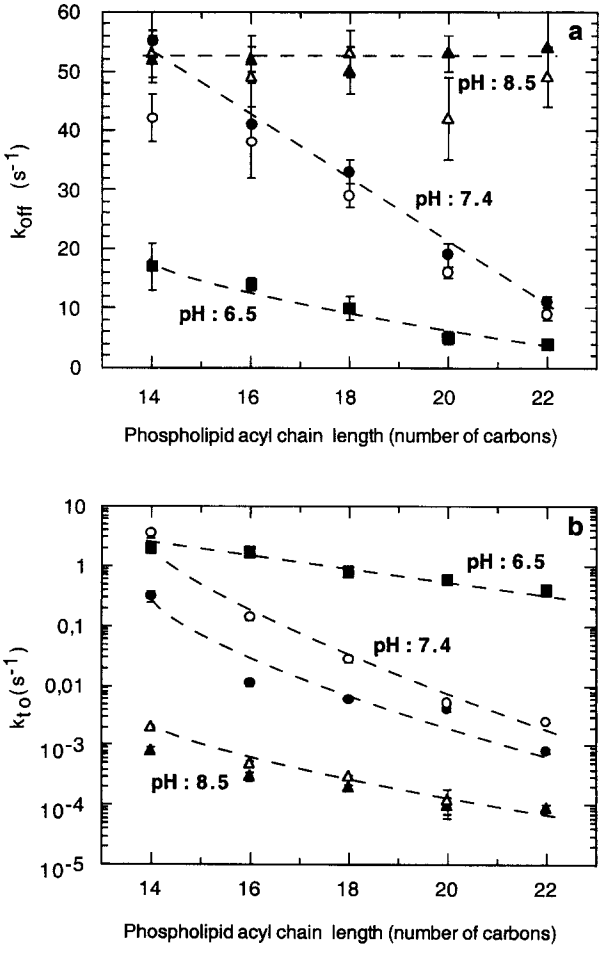

Fig. 4. Effects of bilayer thickness and pH on (a) the exit rate constant k_{off} and (b) the flip-flop rate constant k_{to} as defined in Fig. 1. Temperature: 25°C. Deuteroporphyrin (1×10^{-7} M); ■, pH 6.5, phosphate buffer; ●, pH 7.4, phosphate buffer; ○, pH 7.4, Tris buffer; ▲, pH 8.5, phosphate buffer; △, pH 8.5, Tris buffer. Dashed lines are drawn to better visualize changes, but have no theoretical meaning.

the control of the rate constants. Whereas no dependence of k_{off} on thickness can be seen at pH 8.5, large changes are observed at lower pH values, in particular at pH 7.4. The nature of the buffer has no significant influence on the exit. The small increase of the rate with the phosphate buffer hardly exceeds the uncertainty on the values. The strong dependence of the flip-flop rate constant on the bilayer thickness is illustrated in Fig. 4b. Again, a correlation between the pH and the profile of the changes is observed. Whereas, a fairly smooth decrease of k_{to} is observed at pH 6.5, the decrease is much more abrupt at pH 7.4. Also, at this pH, the

rate greatly depends on the nature of the buffer: for the shortest chain, the value of k_{to} is increased by about one order of magnitude when phosphate buffer is changed to Tris buffer. This effect vanishes for larger chain lengths. At pH 8.5, the effects of both the bilayer thickness and the nature of the buffer are less pronounced.

In order to get more insight into these phenomena, the effect of pH on the rate constants, k_{off} and k_{to}, was investigated in more details for extreme bilayer thickness, i.e. for vesicles made with C14 and C22 phospholipids. The results are shown in Fig. 5.

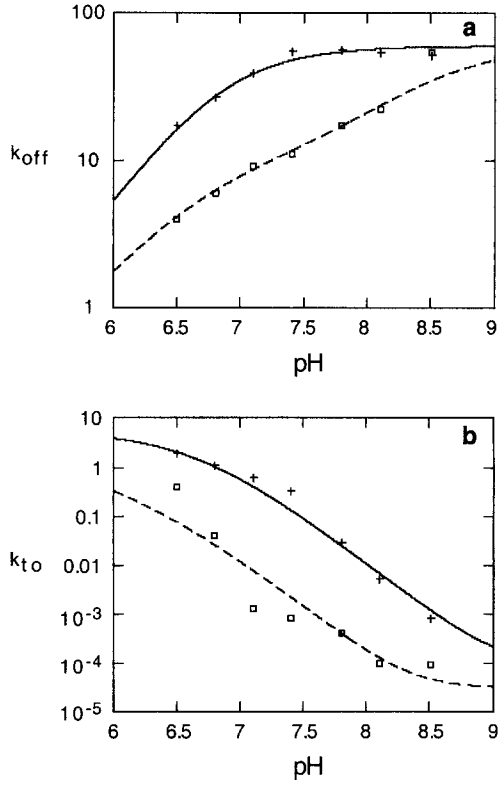

Fig. 5. Effect of pH on (a) the exit rate constant k_{off} and (b) the flip-flop rate constant k_{to} for vesicles made of (+, ——) C14:1-, or (□, – – –) C22:1-phosphatidylcholine. The curves were computed according to Eq. 4 with the following parameters: (a) (+, ——, C14:1); $k_{(0)}$, 0.2; $k_{(-)}$, 15; $k_{(2-)}$, 60; pK_1, 6.9; pK_2, 6.5; (□, – – –, C22:1); $k_{(0)}$, 0.1; $k_{(-)}$, 10; $k_{(2-)}$, 60; pK_1, 8.5; pK_2, 6.7; (b) (+, ——, C14:1); $k_{(0)}$, 5.5; $k_{(-)}$, 1×10^{-3}; $k_{(2-)}$, 1×10^{-4}; pK_1, 6.9; pK_2, 6.4; (□, – – –, C22:1); $k_{(0)}$, 3; $k_{(-)}$, 3×10^{-4}; $k_{(2-)}$, 3×10^{-5}; pK_1, 6.5; pK_2, 5.2. All the rate constants are expressed in s^{-1}.

4. Discussion

Strong lines of evidence from the present study and from previous studies on carboxylic porphyrins [8,14,15,19,26] and related iron complexes [9] indicate that DP incorporates into each hemileaflet of vesicles with its hydrophobic core interacting with the lipid region of the bilayer and its carboxylic chains oriented towards the water interface. As fully discussed earlier [14,15,19,26], this view is supported by the fluorescence spectra of DP that are identical to those of the molecule dissolved in organic solvents, and by the biphasic character of the transfer to albumin indicating the presence of two major porphyrin populations.

The overall affinity of the porphyrin for the vesicles is largely dominated by hydrophobic interactions between the macrocycle core and the phospholipid chains. Indeed, as previously shown [26], the substitution of the hydrogens on the β position of the pyrroles opposite to the carboxylic chains by the more polar $-CH_2(OH)CH_3$ groups, which leads to hematoporphyrin, decreases the affinity by more than one order of magnitude. The protonation of one inner nitrogen, which introduces a positive charge in the center of the macrocycle totally prevents the incorporation within the bilayer [27]. On the other hand, the affinity of the porphyrin for the vesicles remains high even when its carboxylic chains are fully ionized at pH 8.5 (see Table 1). Through the control of the ionization state of these chains, pH has also a major role as illustrated in Figs. 4 and 5. However, a complex interplay between pH and the thickness of the bilayer is observed. It is possible to shed some light on these phenomena by taking into account the hydrophobic profile of membranes that has been investigated in details [20,21]. Such a profile is depicted in Fig. 6.

4.1. Affinity of the porphyrin for vesicles and exchange with the outer medium

If only the outer hemileaflet of the vesicles is populated by the porphyrin, which is the case in our experimental conditions at pH 8.5, the affinity constant K_L is equal to k_{on}/k_{off}. In related systems [16], it was shown that the affinity constant is mainly governed by the value of k_{off}. Indeed, k_{on} was found to be diffusion controlled and little depended on the nature

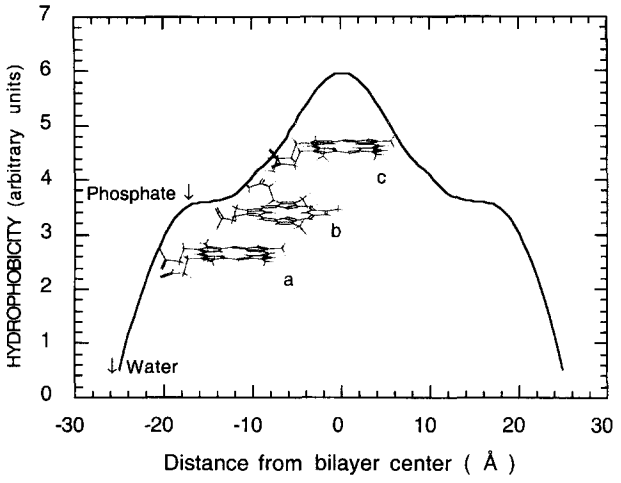

Fig. 6. Full line: typical hydrophobicity profile of a C18:1-phosphatidylcholine bilayer adapted from Subczynski et al. [20]. The energy minimized structures of deuteroporphyrin as dianionic (a), monoanionic (b) and neutral (c) forms are drawn at the same scale as that used for the x-axis. Upon neutralization, the porphyrin is shown to move towards the bilayer center in order to optimize hydrophobic interactions (note that the solid line must not be confused with the phospholipid–water interface).

or the ionization state of the porphyrin. As shown in Table 1 and Fig. 4, neither K_L nor k_{off} were significantly affected by the nature of the phospholipid used, suggesting that the porphyrin remains close to the water interface regardless of the membrane thickness. The charge of the carboxylic chains impede the porphyrin to penetrate deeper into the bilayer. Conversely, the rate for the porphyrin exit is maximum. This localization is illustrated by situation a in Fig. 6. It is worth noting that the expression of K_L as a function of the lipid concentration appears, at least in the present case, to reflect more accurately the physical situation than a partition constant calculated using the volumes of the lipidic and aqueous phases accessible to the porphyrin [11]. The latter representation would lead to changes in the partition constant with the bilayer thickness, which would not reflect the location of the porphyrin at the interface.

When the pH is lowered, successive protonations of the ionized chains lead to the monoanionic and neutral forms. The corresponding pK values have been previously determined to be $pK_1 = 6.0 \pm 0.2$ and $pK_2 = 5.4 \pm 0.2$ in aqueous solutions [26]. Obviously, protonation/deprotonation steps at the interface between the bulk solution and the bilayer need to be considered to fully describe our system from a kinetic point of view. The simplest model would assume that these steps are much faster than the exit of the porphyrin from the bilayer. In that case, the porphyrin can be considered to be always at equilibrium with regard to its protonation state. Then, the system can be described by Eq. 1, except that the intrinsic rate constant k_{off} must be replaced by a global rate constant. This global rate constant would be a combination of the intrinsic rate constants for each form of the porphyrin weighted by its relative abundance. It can be expressed in a general way (the same considerations will apply for k_{to}) as:

$$k = \{k_{(2-)} + k_{(-)} \times 10^{(pK_1 - pH)} + k_{(0)} \times 10^{(pK_1 + pK_2 - 2pH)}\} / \{1 + 10^{(pK_1 - pH)} + 10^{(pK_1 + pK_2 - 2pH)}\} \quad (4)$$

where $k_{(0)}$, $k_{(-)}$ and $k_{(2-)}$ stand for the rate constants relative to the neutral, monoanionic and dianionic forms of the porphyrin, respectively. If the hypothesis holds, the value of k_{off} would depend on pH according to Eq. 4. As shown in Fig. 5, a quite good agreement is found for the vesicles made with C14 chains. Although the equation contains several unknowns to be optimized, the value of k_{off} for the dianionic form can be derived quite precisely from the plateau at higher pH, $k_{off(2-)} = 60 \pm 5\ s^{-1}$. The values for the monoanionic, $k_{off(-)}$, and for the neutral form $k_{off(0)}$, are subjected to much larger uncertainties. They were estimated from manual adjustment of the curve to be around 15 and 0.2 s^{-1}, respectively. As the rate of the porphyrin exit from the bilayer is maximum for the anionic forms, a preferential way for the neutral form exit is likely the loss of protons that are catched by water at the interface. It can be noted that k_{off} is not affected significantly by the nature of the buffer used, contrary to what will be described below for the transfer through the bilayer. As compared to the values obtained in water, the pK of the carboxylic groups were found to be shifted to higher values by about one unit: $pK_1 = 6.9 \pm 0.3$ and $pK_2 = 6.5 \pm 0.3$. A similar shift has been reported for the carboxylic group of stearic acid [28] bound to lipid bilayer. The interactions of DP with vesicles made with saturated C14 chains [14] were very similar to those described here for the unsaturated C14 phospholipids. The dependence of k_{off} versus pH was also found to obey Eq. 4. Similar pK

values (7.2 ± 0.2 and 6.5 ± 0.3) were measured for saturated chains. Thus, in the case of vesicles made with C14 chains, either saturated or unsaturated, it appears that the porphyrin remains in contact with the outer lipid/water interface where it undergoes fast acid-base equilibria.

As evidenced in Fig. 4, the effect of the bilayer thickness on the rate of the porphyrin exit strongly depends on pH. These results can be explained by the degree of burying of the porphyrin within the bilayer modulated by pH. The penetration of the porphyrin in the hydrocarbon heart of the vesicle involves two opposite effects: (1) the energetically favorable optimization of the hydrophobic interactions between the porphyrin core and the lipidic phase of the bilayer; and (2) the unfavorable penetration of the polar carboxylic chains in an environment of low polarity. The magnitude of the latter effect is expected to strongly depend on the charge of the carboxylic chains. The balance between the two effects can be illustrated considering the hydrophobic profile of a membrane. In Fig. 6. is depicted a typical profile drawn from recently published data on C18:1 phospholipids [20] and by using a distance between phosphates of 40 Å [29]. The structure of the porphyrin is drawn using the same scale. A key feature of this profile is its smooth bell-shaped form and the rather small size of the region with maximum hydrophobicity which is, in fact, comparable to that of the porphyrin core. It will be still further narrowed for the C14 phospholipids. As shown in Fig. 6, upon successive neutralizations of the two carboxylic chains, the porphyrin is expected to move towards the center of the bilayer. However, owing to the porphyrin size, optimal hydrophobic interactions between the porphyrin core and the lipidic phase are expected to occur only with the thickest bilayers. It can be expected that the intermediate form, the monoanionic porphyrin, would be particularly sensitive to the balance between hydrophobic and polar forces. In the C22 vesicles this form would be more buried within the bilayer and, as a consequence, it would deprotonate more slowly leading to an increase of apparent pK. As a matter of fact, a shift of the corresponding pK (pH^{-}/P^{2-}) from 6.9 to 8.5 is observed by comparing the C14 and C22 vesicles. However, it must be remembered that as fast acid-base equilibria are not expected to prevail for the C22 vesicles (see below), the notion of pK is only used for the sake of comparison.

It can be noted that these conclusions, inferred from kinetics, are fairly consistent with steady state studies using fluorescence quenching performed by other authors [8,10] on related porphyrins.

An interesting consequence of the interplay between the ionization state of the carboxylic chains and the bilayer thickness is the amplification of their effects. Whereas k_{off} is increased by a factor of about 3 for the C14 vesicles when the pH is increased from 6.5 to 8.5, this factor reaches 14 for the C22 vesicles. In the same line, it must be emphasized that the effect of bilayer thickness is maximum at a pH of 7.4, the physiological value.

4.2. *Transfer of the porphyrin through the bilayer*

As illustrated in Fig. 4b, the rate constant for the transfer of the porphyrin from the inner to the outer hemileaflet of the vesicle span over more than four orders of magnitude. The rate appears to be governed by the hydrophobic barrier formed by the hydrocarbon region. As a matter of fact, the major effect arises from pH changes. When the proportion of the anionic forms of DP is decreased through pH changes from 8.5 to 6.5, the transfer rate is increased by more than three orders of magnitude. Thus, the protonation state of the carboxylic chains governs the rate. At that point, it is important to note that the amount of free protons in the inner aqueous volume of the vesicles is negligible. Using a typical vesicle diameter of 70 nm and a bilayer thickness of 4 nm, it can be calculated that at pH 7, there is less than 1% chance to encounter a proton, whereas the mean number of porphyrin molecules in the inner hemileaflet is 18. In fact, the neutralization of the anionic forms of the porphyrin are under the control of the buffer which is in large excess. At pH 7.4, the ratio between the number of molecules of the acid form of the buffer, $H_2PO_4^-$ for phosphate, $NH_3^+C(CH_2OH)_3$ for Tris, and the number of porphyrin molecules is, on average, 32 and 70, respectively. However, the neutralization does not involve direct interaction between the acid form of the buffer and the porphyrin. Indeed, when the concentration of the Tris buffer was varied from 10 to 50 mM, no change in the rate was observed. Thus, the buffer

appears to play its usual role in keeping the proton activity to a constant level, at least in the time scale of the porphyrin flip-flop. A significant difference is seen between the Tris and phosphate buffers, however. In the case of vesicles made with the short phospholipids, the transfer of the porphyrin is about 10 times faster with the Tris buffer than with the phosphate when the pH in the bulk solution is 7.4. The Tris buffer, an organic compound, may interact with the phospholipid interface. In a lower polarity environment, the $NH_3^+C(CH_2OH)_3$ form of Tris would be less stable resulting in a faster release of protons. As a consequence, the pK of the buffer at the interface and the local pH would be decreased. Owing to its more polar character, less interaction is expected between phosphate and the phospholipid interface.

As shown in Fig. 5, in the case of C14:1 vesicles, the value of k_{to} depends on pH according to Eq. 4. The best fit of the experimental data led to $k_{to(0)} = 5.5 \pm 1.0\ s^{-1}$. The values of $k_{to(-)}$ and $k_{to(2-)}$ were estimated to be around 1×10^{-3} and 1×10^{-4} s^{-1}, respectively. It can be noted that the pK values derived from this fit, $pK_1 = 6.9 \pm 0.3$ and $pK_2 = 6.4 \pm 0.3$ are very similar to those obtained from the dependence of k_{off} on pH. Thus, the porphyrin remains in contact with the inner phospholipid interface, where it undergoes fast acid-base equilibria, in the same way it was found for the outer interface. On the other hand, when the bilayer thickness was increased, the fit of k_{to} by Eq. 4 was quite poor as illustrated for the C22 vesicles (Fig. 5). The porphyrin becoming more embedded in the bilayer, especially the monoanionic form (see Fig. 6, location b), was less accessible to protons. The curve of k_{to} versus pH was shift to low pH, accordingly.

The mechanism of the porphyrin permeation through the bilayer can be tentatively analyzed in terms of the solubility–diffusion mechanism [30], although this model which is based on the existence of a linear concentration gradient across the bilayer appears to be best suited to permeation of smaller molecules. According to this mechanism, the permeability of molecules is expected to moderately decrease when the bilayer thickness increases which is observed in Fig. 4, at least if we consider the extreme pH values, 6.5 and 8.5. At intermediate pH, the complex interplay between hydrophobic interactions and the protonation of the porphyrin carboxylate chains, as described above, leads to an amplification of the effect of the bilayer thickness.

The combined effects of pH and membrane thickness outlined in this paper are likely to be important determinants of the membrane transport of carboxylic porphyrins used in photodynamic therapy. These results have also evident bearing on the final steps of heme metabolism which involves membrane transport of protoporphyrin, a dicarboxylic porphyrin related to deuteroporphyrin, and its iron complex. The amplification, at physiological pH, of the effect of membrane thickness on the flip-flop and exit rates of the porphyrin is of major importance. This suggests that the membrane transport of such molecules may depend, to an unexpected extent, on the lipid composition of the bilayer in addition to phase boundary effects [31]. Also, interactions of the membrane with proteins or peptides that can lead to bilayer thinning [32,33] may come into play.

Acknowledgements

This work is a contribution from Institut Féderatif de Recherche No. 63 and was supported by a grant from MESR to N.M. and by Grant 7209 from ARC. We thank Dr. G. Barratt (Université Paris-Sud, CNRS URA 1218, Chatenay-Malabry, France) for her help in vesicle size determination.

References

[1] J.D. Spikes, Photodynamic reactions in photomedicine, in: J.D. Regan, J.A. Parrish (Eds.), The Science of Photomedicine, Plenum Press, New York, 1982, pp. 113–144.
[2] T.J. Dougherty, W.R. Potter, D. Bellnier, Photodynamic therapy for the treatment of cancer: current status and advances, in: D. Kessel (Ed.), Photodynamic Therapy of Neoplastic Disease, Vol. 1, CRC Press, Boston, USA, 1990, pp. 1–19.
[3] B.W. Henderson, T.J. Dougherty, Photochem. Photobiol. 55 (1992) 145–157.
[4] J. Moan, K. Berg, Photochem. Photobiol. 53 (1991) 549–553.
[5] K.W. Woodburn, N.J. Vardaxis, J.S. Hill, A.H. Kaye, J.A. Reiss, D.R. Phillips, Photochem. Photobiol. 55 (1992) 697–704.
[6] M. Dellinger, Photochem. Photobiol. 64 (1996) 182–187.

[7] D. Kessel, Y. Luo, Y. Deng, C.K. Chang, Photochem. Photobiol. 65 (1997) 422–426.
[8] F. Ricchelli, G. Jori, S. Gobbo, M. Tronchin, Biochim. Biophys. Acta 1065 (1991) 42–48.
[9] J.B. Cannon, F.S. Kuo, R.F. Pasternack, N.M. Wong, U. Muller-Eberhard, Biochemistry 23 (1984) 3715–3721.
[10] E. Gross, B. Ehrenberg, Biochim. Biophys. Acta 983 (1989) 118–122.
[11] W.R. Light, J.S. Olson, J. Biol. Chem. 265 (1990) 15623–15631.
[12] W.R. Light, J.S. Olson, J. Biol. Chem. 265 (1990) 15632–15637.
[13] M.Y. Rose, R.A. Thompson, W.R. Light, J.S. Olson, J. Biol. Chem. 260 (1985) 6632–6640.
[14] K. Kuzelova, D. Brault, Biochemistry 34 (1995) 11245–11255.
[15] K. Kuzelova, D. Brault, Biochemistry 33 (1994) 9447–9459.
[16] C. Vever-Bizet, D. Brault, Biochim. Biophys. Acta 1153 (1993) 170–174.
[17] F. Frézard, A. Garnier-Suillerot, Biochim. Biophys. Acta 1389 (1998) 13–22.
[18] M. Rotenberg, S. Cohen, R. Margalit, Photochem. Photobiol. 46 (1987) 689–693.
[19] D. Brault, J. Photochem. Photobiol. B: Biol. 6 (1990) 79–86.
[20] W.K. Subczynski, A. Wisniewska, J.J. Yin, J.S. Hyde, A. Kusumi, Biochemistry 33 (1994) 7670–7681.
[21] O.H. Griffith, P.J. Dehlinger, S.P. Van, J. Membr. Biol. 15 (1974) 159–192.
[22] B.A. Lewis, D.M. Engelman, J. Mol. Biol. 166 (1983) 211–217.
[23] M. Dellinger, D. Brault, J. Chromatogr. 422 (1987) 73–84.
[24] F. Olson, C.A. Hunt, F.C. Szoka, W.J. Vail, D. Papahadjopoulos, Biochim. Biophys. Acta 557 (1979) 9–23.
[25] L.D. Mayer, M.J. Hope, P.R. Cullis, Biochim. Biophys. Acta 858 (1986) 161–168.
[26] D. Brault, C. Vever-Bizet, T. Le Doan, Biochim. Biophys. Acta 857 (1986) 238–250.
[27] D. Brault, C. Vever-Bizet, K. Kuzelova, J. Photochem. Photobiol. B: Biol. 20 (1993) 191–195.
[28] M. Egret-Charlier, A. Sanson, M. Ptak, O. Boulousa, FEBS Lett. 89 (1978) 313–316.
[29] M.C. Wiener, S.H. White, Biophys. J. 61 (1992) 434–447.
[30] R.B. Gennis, Interactions of small molecules with membranes: partitioning, permeability, and electrical effects, in: Biomembranes: Molecular Structure and Function, Springer, New York, 1989, pp. 235–269.
[31] T.-X. Xiang, B.D. Anderson, Biochim. Biophys. Acta 1370 (1998) 64–76.
[32] S. Ludtke, K. He, H. Huang, Biochemistry 34 (1995) 16764–16769.
[33] Y. Wu, K. He, S.J. Ludtke, H.W. Huang, Biophys. J. 68 (1995) 2361–2369.